Journal of Biomedical Optics 5(3), 330–337 (July 2000)

Methodology for examining polarized light interactions with tissues and tissuelike media in the exact backscattering direction

Ryan C. N. Studinski
McMaster University
Department of Physics
Hamilton, ON, Canada L8S 4M1

I. Alex Vitkin
Ontario Cancer Institute/University of Toronto
Department of Medical Biophysics
and Radiation Oncology
Toronto, ON, Canada M5G 2M9

Abstract. The properties of polarized light emerging from turbid media in the exact backscattering direction are studied by modulating the incident light polarization state and isolating the synchronous signal with lock-in amplifier detection. The results are reported for polystyrene microsphere suspensions in distilled water, with and without glucose, and for both *ex vivo* and *in vivo* biological tissues. A new theoretical formulation based on Mueller calculus is developed to describe the observed behavior of the backscattered light in terms of two sample parameters: optical rotation and depolarization. This technique proved successful in modeling both phantom and tissue samples. Results showed the presence of a significant surviving polarization fraction in the backscattering direction even in extremely dense optical phantom media, an important finding that has not been observed at other detection angles. Substantial polarized light preservation in biological tissue samples is also demonstrated for this detection geometry. This illustrates the potential of using polarized light to investigate turbid biological materials *in vivo* in retroreflection geometry. [S1083-3668(00)00603-1]

Keywords: polarization; backscattering; turbidity; chirality; polarization modulation.

Paper 990055 JBO received Oct. 15, 1999; revised manuscript received Feb. 4, 2000; accepted for publication Feb. 14, 2000.

1 Introduction

The use of optical methods to study heterogeneous turbid media has generated interest due to its many potential applications, which include such diverse fields as astrophysics, ocean and atmospheric optics, and biomedical optics. Generally, as light passes through a turbid material, it follows a tortuous path and scatters many times (diffuse multiple scattering). Consequently, its direction, polarization and coherence are randomized, and potentially useful information that may have been encoded in these properties is lost. Conversely, if the light travels a relatively direct and short route through the medium and is weakly scattered (ballistic or ''snake'' photons), its various properties are maintained to an extent. However, unless the turbid sample is weakly scattering and optically thin, the majority of the light will emerge with these properties scrambled; in general, the small fraction of information-containing photons must be separated from the information-degrading randomized light for the best estimate of turbid medium characteristics. This is what makes it difficult to use light-based methods to do quantitative analysis of multiply scattering materials.

Address correspondence to I. Alex Vitkin, Department of Medical Biophysics, Ontario Cancer Institute/University of Toronto, 610 University Avenue, Toronto, ON, Canada M5G 2M9. Electronic mail: vitkin@oci.utoronto.ca

An example of a turbid material of interest is mammalian tissue. It is a highly scattering medium for light of wavelengths between 600- and 1300 nm,[1] so studying it optically is a challenging task. Novel methods of spatial imaging and mapping in tissues include time-of-flight gating, frequency-domain amplitude modulation, continuous-wave transillumination,[2] low-coherence tomography,[3] and confocal microscopy.[4] Optical methods of composition analysis often use spectral measurements, whereby optical signals at discrete wavelengths or over a particular wavelength range are analyzed to determine the presence, concentration, and perhaps distribution of particular constituents.[5] Both the imaging and spectroscopic investigations are hindered by the effects of multiple scattering.

Among the methods available to analyze turbid media, the use of polarized light has attracted much attention recently, as it has been discovered that multiply scattered photons still maintain partial polarization.[6–16] A typical experiment entails launching a known polarization state in light into a turbid sample and measuring the polarization properties of the remitted light. The detected signal depends on many variables, including the number and nature of scattering events, the incident polarization state, and the detection geometry. With

1083-3668/2000/$15.00 © 2000 SPIE

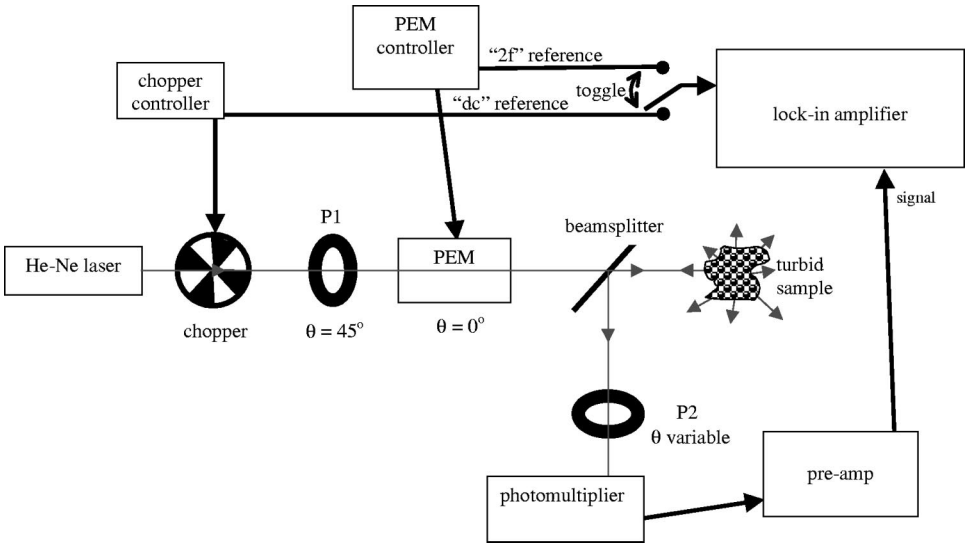

Fig. 1 Schematic of the experimental system for measuring diffusely backscattered polarized light.

respect to the latter variable, it has been shown that for sufficiently dense optical media, the emergent light is completely depolarized.[12–14] However, this may be different in one particular direction, that at 180° to the incident beam,[6–11,15,16] and one of the goals of the present study is to quantify the polarization behavior of optically thick biological media in this geometry.

There are other factors that can influence the behavior of the polarized light, for example the presence of optically active, or chiral, molecules. Probably the best known chiral molecule, and one of paramount biological importance, is glucose. Chiral molecules have indices of refraction which differ for left and right circular polarization states, one manifestation of which is rotation of the linear component of polarized light. This has been utilized extensively in transparent materials (such as dilute protein suspensions) in polarization measurements of the concentration of chiral molecules.[17] The effect of chiral molecules on polarized light propagation in multiply scattering media has been studied,[12,14,18,19] with an important finding that they reduce the rate of light depolarization.

Previous work has shown, both theoretically and experimentally, that polarized light emerging in most directions from a multiply scattering sample will inevitably lose its polarization if the turbid sample is sufficiently optically dense.[12–14] Thus, detected light in those directions would have limited applications for polarization analysis of optically thick media. If polarized light were to be used on human tissue, a detection geometry of particular interest from the standpoint of clinical convenience would be in the backscattering direction, and studies at this detection angle deserve further investigation. If some of the light retained its polarization properties upon multiple scattering, as studies at 180° suggests,[6–11,15,16] and this effect could be quantified and exploited, potentially useful measurements could be made in almost any clinical situation. For example, one of the most important potential biomedical applications of such a system would be to detect glucose *in vivo* noninvasively. Since light in the visible and infrared regions of the electromagnetic spectrum is not harmful to biological tissues at moderate fluence levels, has a penetration depth of several millimeters, and has a reasonable chance of scattering out of the tissue and being detected, it would be ideal for making noninvasive measurements. Other practical reasons for studying the behavior of light at 180° would be for the possibility of spatial imaging to map out the locations of sample structures and compositions,[20] and to gain a better general understanding of turbid systems.

2 Theory

The current study makes use of the photoelastic modulator (PEM)[21] for polarization modulation of the incident beam, with synchronous detection of the light multiply scattered from a turbid medium. This arrangement enables the detection of a small polarization-maintaining fraction among a background of mostly depolarized light, such as the case after interacting with a turbid sample. The PEM consists of a transparent amorphous quartz block, driven to oscillate at a resonant frequency of 50 kHz by a piezoelectric transducer. The resultant linear birefringence induced in the quartz imparts a time-variable retardation between the components of the electric field of the transmitted beam that are perpendicular and parallel to the axis of modulation.[22] The magnitude of the maximum retardation, and thus the extreme polarization states furnished to the passing beam in an oscillation cycle, are selected by the user.

Figure 1 illustrates the setup for the experiment. The beam is polarized by a linear polarizer, passes through the PEM, transmits through a beamsplitter, and scatters in the sample; the fraction scattered at 180° with respect to the incident beam reflects off the beamsplitter, passes through another polarizer, and impinges on the detector. In order to describe the polarization behavior of this setup, Mueller calculus is used.[23] Each optical element is represented by a 4×4 matrix which models the effect of the element on polarized light, the polarization state of the latter being represented by a 4×1 Stokes vector. The linear polarizers, P1 and P2, can be both represented by

$$\mathrm{P1,P2}=\begin{bmatrix} 1 & \cos 2\theta & \sin 2\theta & 0 \\ \cos 2\theta & \cos^2 2\theta & \sin 2\theta \cos 2\theta & 0 \\ \sin 2\theta & \sin 2\theta \cos 2\theta & \sin^2 2\theta & 0 \\ 0 & 0 & 0 & 0 \end{bmatrix}, \tag{1}$$

where θ is the angle of the pass axis with respect to the optical plane, here defined as the horizontal surface of the optical table. For the current study, P1 is oriented at 45° to the optical plane, whereas the orientation of P2 is varied over a total θ range of 180°. Thus, θ in the final expression is the variable orientation of P2 with respect to the horizontal.

The Mueller matrix for the photoelastic modulator, with its modulation axis horizontal (0°), contains terms that are functions of δ, the retardation setting of the PEM:

$$\mathrm{PEM}=\begin{bmatrix} 1 & 0 & 0 & 0 \\ 0 & 1 & 0 & 0 \\ 0 & 0 & \cos(\delta) & -\sin(\delta) \\ 0 & 0 & \sin(\delta) & \cos(\delta) \end{bmatrix}. \tag{2}$$

The beamsplitter, positioned at 45° with respect to the incident beam direction, contributes two different matrices to the theoretical formulation.[23] One matrix ($\mathrm{BS_{trans}}$) represents the light transmitted through the beamsplitter on route to the sample; the other ($\mathrm{BS_{refl}}$) represents the light reflected by the beamsplitter from the sample toward the detector

$$\mathrm{BS_{trans}}=\begin{bmatrix} \cos^4(r-I)+1 & \cos^4(r-I)-1 & 0 & 0 \\ \cos^4(r-I)-1 & \cos^4(r-I)+1 & 0 & 0 \\ 0 & 0 & 2\cos^2(r-I) & 0 \\ 0 & 0 & 0 & 2\cos^2(r-I) \end{bmatrix}, \tag{3a}$$

$$\mathrm{BS_{refl}}=\begin{bmatrix} 1 & \sin 2r & 0 & 0 \\ \sin 2r & 1 & 0 & 0 \\ 0 & 0 & -\cos 2r & 0 \\ 0 & 0 & 0 & -\cos 2r \end{bmatrix}, \tag{3b}$$

where I is the angle of the beamsplitter with respect to the plane perpendicular to the path of the laser (45° in the setup used for this experiment), and r is the angle of refraction within the beamsplitter as calculated by Snell's law. While the presence of the beamsplitter complicates the resultant mathematics, and necessitates additional experimental care in making the actual measurements, it does enable detection of the scattered light in the exact retroreflection geometry. Other methods, such as the use of isocentric pivoting[14,20,24] or apertured mirror,[25,26] cannot detect the signal at 180° to the incident beam.

The matrix used to represent the sample was modeled as a combination of circular birefringence and depolarization. Specifically, the amount of optical rotation created by the sample is denoted by α, and the amount of polarization retained is denoted by β. It was taken to be the product of a depolarization matrix,[27] a rotation matrix, and a reflection matrix. While in general matrices do not commute, the effect of varying the order of the matrices only changes the sign of the parameter α (i.e., α becomes $-\alpha$) and this is not important for the current study. The resultant sample matrix is

$$\begin{aligned}\mathrm{Sample}=&\begin{bmatrix} 1 & 0 & 0 & 0 \\ 0 & \beta & 0 & 0 \\ 0 & 0 & \beta & 0 \\ 0 & 0 & 0 & \beta \end{bmatrix} \\ &\cdot\begin{bmatrix} 1 & 0 & 0 & 0 \\ 0 & \cos 2\alpha & \sin 2\alpha & 0 \\ 0 & -\sin 2\alpha & \cos 2\alpha & 0 \\ 0 & 0 & 0 & 1 \end{bmatrix} \\ &\cdot\begin{bmatrix} 1 & 0 & 0 & 0 \\ 0 & 1 & 0 & 0 \\ 0 & 0 & -1 & 0 \\ 0 & 0 & 0 & -1 \end{bmatrix} \\ =&\begin{bmatrix} 1 & 0 & 0 & 0 \\ 0 & \beta\cos 2\alpha & \beta\sin 2\alpha & 0 \\ 0 & \beta\sin 2\alpha & -\beta\cos 2\alpha & 0 \\ 0 & 0 & 0 & -\beta \end{bmatrix}. \end{aligned} \tag{4}$$

To predict the operation of the system, the matrices are multiplied together with S_{initial}, as follows:

$$S_{\mathrm{final}}=[\mathrm{P2}][\mathrm{BS_{refl}}][\mathrm{Sample}][\mathrm{BS_{trans}}][\mathrm{PEM}][\mathrm{P1}]S_{\mathrm{initial}}. \tag{5}$$

The first term of the resultant Stokes vector S_{final} represents the final intensity of the light reaching the detector, and thus constitutes the measured signal. It contains variable retarda-

tion expressions of the form $\cos(\delta)=\cos(\delta_m \cdot \sin[2\pi ft])$, that can be expanded as a Fourier–Bessel series[28] into constant and oscillatory terms

$$\cos[\delta_m \sin(2\pi ft)] = J_0(\delta_m) + 2J_2(\delta_m)\cos(4\pi ft) + \cdots, \tag{6}$$

where J_0 and J_2 are the zeroth and second order Bessel functions of the first kind, respectively. This indicates that there are constant (dc) and oscillatory (ac) components in the signal. Normalizing the ac signal component at twice the PEM's modulation frequency by the dc contribution eliminates unimportant experimental constants, yielding

$$\frac{2f}{\mathrm{dc}} = \frac{2J_2(\delta_m)A}{J_0(\delta_m)A + B + C}, \tag{7a}$$

where

$$\begin{aligned} A &= 2\beta\cos^2(r-I)(\sin\alpha\sin 2r + \sin\alpha\cos 2\theta \\ &\quad + \sin 2\theta\cos 2r\cos\alpha), \\ B &= [\cos^4(r-I)+1](1+\cos 2\theta\sin 2r) \\ C &= \beta[\cos^4(r-I)-1][(\sin 2r+\cos 2\theta)\cos\alpha \\ &\quad - \sin 2\theta\cos 2r\sin\alpha]. \end{aligned} \tag{7b}$$

In the reported experiments, with $I=45°$ and $r=27.3°$ (Snell's law with $n_{BS}=1.54$), Eq. (7b) becomes:

$$\begin{aligned} A &= 1.82\beta(0.82\sin\alpha + \sin\alpha\cos 2\theta + 0.58\cos\alpha\sin 2\theta), \\ B &= 1.82(1+0.82\cos 2\theta), \\ C &= -0.18\beta[(0.82+\cos 2\theta)\cos\alpha - 0.58\sin 2\theta\sin\alpha]. \end{aligned} \tag{7c}$$

These expressions can be fitted to experimental data by varying α and β, the unknown sample properties at a selected PEM retardation δ_m. This is accomplished by using θ as the independent variable and minimizing the discrepancy, in the least-squared sense, between the measured $(2f/\mathrm{dc})$ ratios and the theoretical prediction of Eq. (7) in a nonlinear two parameter fit.

3 Experimental Methods

Figure 1 shows the layout of the experiment. The light from a helium–neon laser ($\lambda = 632.8$ nm) passes through a mechanical chopper, to allow the dc light level to be read sensitively with the lock-in amplifier. It then passes through linear polarizer (P1), fixed at 45° with respect to the horizontal plane, and traverses the transparent oscillating quartz element of the photoelastic modulator that imparts a relative phase to the orthogonal components of the transmitted beam. The PEM's axis of the modulation is horizontal. The PEM is known to cause interference effects with monochromatic light sources via multiple reflections off the surfaces of the quartz element which can compromise the sample signal.[29] Thus, the PEM was angled in the optical plane at ~8° with respect to the light propagation direction, to direct the interference light away from the sample beam path.

Upon emerging from the PEM, the light strikes a beamsplitter, angled in the optical plane at 45° with respect to the incident beam direction. The reflected portion hits a beam dump and is no longer used. The transmitted portion travels to the turbid chiral sample and is scattered in many directions; the backscattered light to be detected travels back to the beamsplitter. The reflected portion of this fraction of light is incident on a second linear polarizer (P2). The angle θ of this polarizer with respect to the horizontal is varied during the measurement, and its values are used in fitting the theory of Eq. (7) to the data. After passing through the second polarizer, the beam impinges on a photomultiplier detector. Based on its sensitive area and the detector–beamsplitter–sample separation, the cone of acceptance around the exact backscattering direction was 15 mrad. The signal from the photomultiplier is a photocurrent, which is converted into a voltage by a transimpedance preamplifier. The resultant voltage is read out by a lock-in amplifier. The lock-in amplifier's reference frequency is set to either twice the frequency of the photoelastic modulator ($2f$) or the frequency of the mechanical chopper (dc) by a toggle switch. The voltages at both these frequencies are measured for any given angle of P2 and the two signals are ratioed. The PEM setting was $\delta_m = 3.469$ radians in order to maximize the amplitude of the $2f/\mathrm{dc}$ ratio.[14] After correction factors are applied (to account for the chopper blocking half the light, and the lock-in amplifier measuring rms instead of peak-to-peak voltage), $2f/\mathrm{dc}$ values are input into the nonlinear regression analysis package (SigmaPlot 3.0), and Eq. (7) is fitted to the data with α and β as the fitting parameters optimized to minimize the sum of the squared differences between theory and data.

Several types of samples were used in the experiments. A mirror was used for calibration, positioned perpendicular to the path of the beam. Liquid samples consisting of polystyrene microspheres (diameter = 1.4 μm) and glucose in distilled water were contained in a rectangular (1 cm × 1 cm) optical-grade quartz cuvette. The cuvette was angled slightly so that the specularly reflected spot did not project back towards the detector, to ensure that scattered light emerging from the sample itself dominated the measurements. Samples of ground meat were contained in a plastic cuvette with a 4-mm-diam aperture, so the light could reach the sample, and escape in the backward direction, without interacting with a container surface. Finally, human tissue was measured *in vivo* by having a volunteer place his/her hand in the path of the beam. The palm of the hand rested on a platform to maintain stability. The measurement was in the region between the thumb and index finger, as it was the most comfortable and stable way to position the hand. All measurements were performed at room temperature.

4 Results

To test the validity of the theory and the performance of the equipment in the retroreflection configuration, a mirror signal was measured, as its effects on polarized light could be predicted. It should produce no rotation of the polarized light ($\alpha = 0$) and no depolarization ($\beta = 1$). The result of a typical measurement is shown in Figure 2. The points represent corrected ratios, while the solid line is the theoretical best fit. The fit for the curve is excellent ($R^2 = 0.999$), with optimum pa-

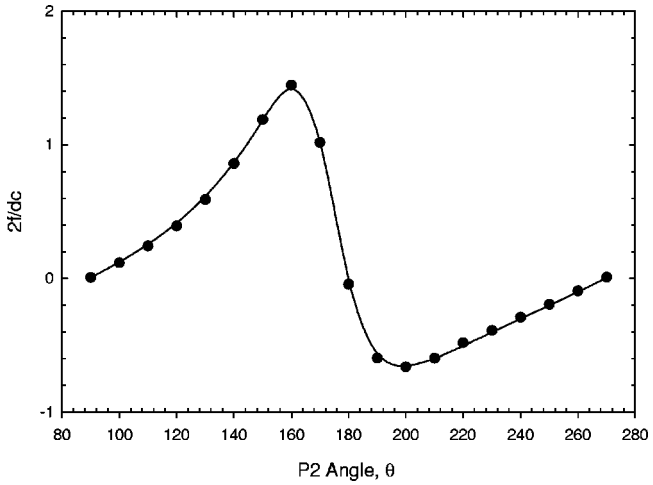

Fig. 2 Initial calibration of the system, with mirror as the scattering sample. The points are the corrected 2 *f*/dc values and the solid line is the theoretical best-fit predicted by Eq. (7). The R^2 for the fit is 0.999 and the predicted α and β are $+0.1° \pm 0.3°$ and 1.00 ± 0.01, respectively.

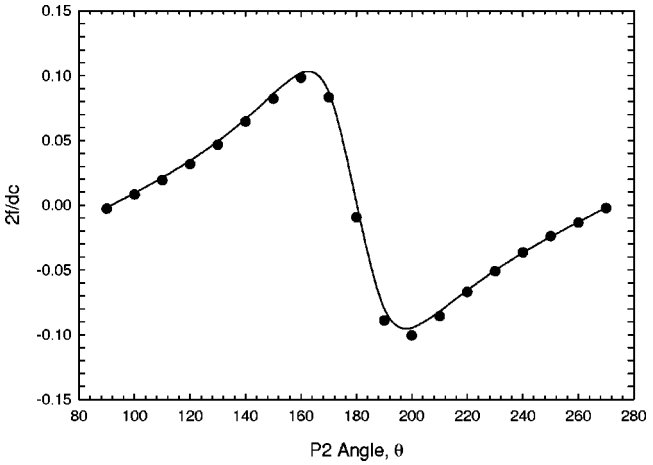

Fig. 3 A typical data set measured from a microsphere suspension containing 1.5% (w/v) of 1.4 μm diam microspheres and no glucose. The best-fit values of α and β are $1.1° \pm 0.7°$ and 0.11 ± 0.01, respectively, with $R^2 = 0.995$.

rameters $\alpha = +0.1° \pm 0.3°$ and $\beta = 1.00 \pm 0.01$, in good agreement with the expected values. This result validated the accuracy of the methodology and ensured that all the equipment, both optical and electronic, was working as predicted. Repeated measurements of the mirror, used as a periodic calibration check, produced fits that were consistently excellent ($R^2 \geqslant 0.99$), with the resultant α and β close to their expected values. The amount of error in each measurement was small, yielding the best fit values with excellent reproducibility.

Measurements were then made with polystyrene microspheres suspended in glucose solution. Detailed results of microsphere scattering in the exact retroreflection direction will be published elsewhere. Presently, only preliminary major trends are reported. Measurements were made with a wide variety of liquid suspensions, containing different concentrations of microspheres and glucose. Typical results measured from a turbid sample without glucose and a microsphere concentration of 1.5% (w/v) are shown in Figure 3. The resultant fits yield $\alpha = 1.1° \pm 0.7°$ and $\beta = 0.11 \pm 0.01$. As shown, samples consisting of microspheres produce fits which are quite good, although not as consistently excellent as the fits from the mirror sample. The values of α and β are also realistic (i.e., β is non-negative and is less than unity, and α is not a number of unreasonably large magnitude). This is strong evidence that the measurement method and the derived theory are able to describe the behavior of polarized light in a scattering medium. Both the mirror and the polystyrene microsphere solutions yield very precise β values, and less precise α values. Investigations into improving the precision of α are currently underway.

An important finding emerging from the study of microsphere suspensions is shown in Figure 4. It displays β as a function varying concentrations of microspheres for samples with and without glucose. It appears that polarized signals survive in the exact backscattering direction even in very scattering media. This is to be contrasted with the results of previous studies[12–14] of light emerging in other directions that show the degree of polarization approaching zero as the optical thickness increases approximately 10–15 transport mean free paths. For comparison, the ranges of scattering properties in Figure 4, as calculated according to Mie theory,[30] are: scattering coefficient $= 34–600\ \text{cm}^{-1}$, transport scattering coefficient $1.8–38.5\ \text{cm}^{-1}$, transport mean free path 0.55–0.026 cm (~2–40 transport mean free paths). Additional measurements not included on the graph were in the 2%–3% microsphere concentration range, still showing β values around 0.11. Finally, a suspension containing 17% microspheres (~400 transport mean free paths) and no glucose yielded $\alpha = 0.2° \pm 1.1°$ and $\beta = 0.073 \pm 0.002$, further illustrating that in even extremely optically dense and highly scattering conditions, a certain amount of polarization is maintained. A possible explanation for the enhanced survival of the polarization is the constructive interference between a multiply scattered wave and its time reversed conjugate which follows the same path,

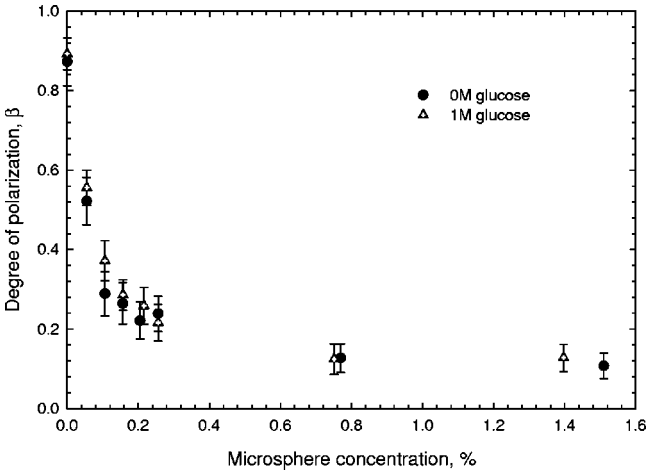

Fig. 4 Degree of polarization as a function of increasing turbidity of the polystyrene microsphere suspension, in the presence and absence of glucose. For both systems, the curves seem to plateau to nonzero levels even in the limit of very high scattering.

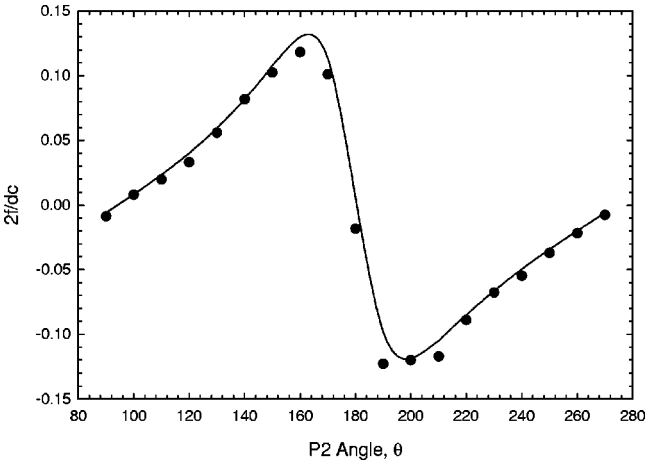

Fig. 5 Polarization data with best-fit line, obtained from a hand of a Caucasian volunteer. The R^2 value for the fit is 0.98 and the derived α and β are $+2.7° \pm 1.3°$ and 0.14 ± 0.01, respectively.

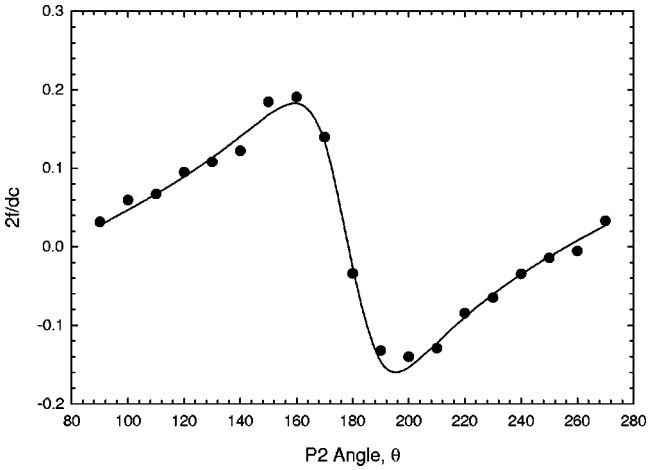

Fig. 6 Polarization data with best-fit line, measured from a ground beef sample. The R^2 is 0.99 and the predicted α and β are $-9.0°$ $\pm 1.0°$ and 0.19 ± 0.01, respectively.

a phenomenon referred to as weak localization.[6–11,15,16] This is an important experimental result as it shows that there will be a finite fraction of polarization maintained in retroreflection, which may allow applications of this method in highly scattering media.

The second feature evident from Figure 4 is that, within experimental error, the depolarization rates with and without glucose are similar to each other. This backscattering result differs from observations at other detection angles, where the glucose-dependent enhancement of polarization has been reported.[12,14,19] The enhancement may still be present yet remain undetected by the current methodology, but evidently its magnitude in retroreflection is much lower than in other detection directions.

Figure 5 shows the results from a hand of a human volunteer. The results of the fit ($R^2 = 0.98$) yielded $\alpha = +2.7° \pm 1.3°$ and $\beta = 0.14 \pm 0.01$. From repeated measurements, and from additional experiments with three more volunteers, β values were reproducible to within $\pm 10\%$, and were in the 0.12–0.14 range for the four people studied. The reproducibility is remarkably good, considering the noise from the inevitable small movements during the measurement process. Given the excellent reproducibility in the degree of polarization determination, we tentatively interpret the variation in the measured β values as true indications of the intersample differences, such as differences in anatomy and physiology in the hands of the different subjects. Clearly, much additional work is required to further elucidate this association. All reported measurements were from the hands of Caucasian volunteers, and we are currently examining the effect of different skin pigmentation and microstructure on the polarization measurements. The optical rotation results exhibit unacceptably large errors and do not seem to be reproducible at present. It is worth noting, however, that many of the hand measurements yielded relatively large α values of 6°–8°. This indicates a large amount of optical rotation in the measurements, which may be useful for detecting chiral molecules *in vivo*, *provided* the precision and reproducibility in α results can be improved. Note that the possible influence of tissue linear birefringence is not taken into account in this analysis. This issue is further addressed in Sec. 5.

Measurements were also made with ground beef samples, shown in Figure 6. This particular measurement was best described by $\alpha = -9.0° \pm 0.9°$ and $\beta = 0.19 \pm 0.01$. This was the first sample that resulted in a large optical rotation of opposite sense. The sign of the rotation, and less so the magnitude, was reproducible on repeated measurements of different ground beef samples. We are currently investigating the significance of this observation. Once again, β was reproducible to better than $\pm 10\%$.

In experiments with these biological tissues, as well as with the *in vivo* measurements reported above, there were large fluctuations ($\pm 15\%$–30%) in the magnitude of the 2 f signal. As the effect was initially observed in the hand samples, the first noise source suspected was sample motion. However, since the same amount of noise was seen with the meat samples which were motionless, that was ruled out. Despite this noise, and whatever its cause, good fits ($R^2 \geq 0.94$) were obtained with both *in vivo* and *ex vivo* tissues, possibly because of the utility of the signal ratio procedure.

5 Discussion

The methodology for detection and analysis of polarized light backscattered from turbid media has been tested in microsphere phantoms and in biological tissues. The method is capable of furnishing two important measures of sample interaction with polarized light: the optical rotation of the linearly polarized fraction, and the degree of polarization.

The results from microsphere suspension studies suggest that the developed model is appropriate for describing the behavior of the backscattered polarized light. An important finding is that at exceedingly large optical densities, the amount of polarization retained plateaus to a value above zero, instead of diminishing completely as it does at other observation angles. This plateau appears to be in the range of $\beta = 0.07$–0.12. It is also shown that, unlike in other detection directions, glucose does not cause a noticeable increase in the amount of polarization retention in turbid suspensions. In ad-

dition to furnishing useful information about the turbid microsphere system, these results suggest that the developed experimental and theoretical methodology may be well suited for further polarization studies of turbid chiral and achiral media in the backscattering direction.

The ability to detect a polarized fraction in diffusive backscattering from *in vivo* tissues is extremely encouraging. The implication is that polarized light may provide a useful means of studying heterogeneous turbid biological materials. This possibility is further strengthened by the fact that similar results were obtained by working with samples of *ex vivo* homogenized beef. The outcome of the tissue experiments is all the more important since it has been reported that phantoms such as microsphere suspensions do not interact in the same way as biological tissue with polarized light,[31] and so the use of microsphere phantom data to model tissue may be inappropriate.

It is important to note that the results from Figures 5 and 6 show that the developed theory can be used to describe polarized light scattering from biological samples. However, biological tissues possess additional properties, for example linear birefringence, which have not been included in the current formulation. In other words, real tissues are not only circularly birefringent and multiply scattering, but likely exhibit direction-dependent linear birefringence as well. So the values of α and β computed with the current theory may be inaccurate. However, an important feature evident from the analysis of both the *in vivo* and *ex vivo* samples is the good quality of the fits and their reasonable reproducibility (comparable to the microsphere system that *does not* exhibit linear birefringence). Thus, the described methods may be yielding slightly inaccurate optical rotation and preserved polarization values, but they nevertheless appear appropriate for the tissue work. Theoretical improvements in progress are expected to further improve the accuracy of the model.

The degree of polarization parameter is determined with an excellent degree of precision and reproducibility in both microsphere and tissue measurements. It is mostly sensitive to the path length traveled by the photons, with a smaller β indicating a longer path length, but it may also be affected by the presence of chiral molecules. As well, it may depend on the ''tortuosity'' of the path taken by the photons. The error seen in the β parameter is not seriously affected by the presence of occasional outlier points, and good fits are obtained even with noisy data sets. As a result, trends in degree of polarization can be measured reliably. This provides a useful diagnostic, largely unaffected by noise, for analysis of turbid media.

At present, we are unable to get precise measurements of optical rotation at the exact backscattering direction. For example, for the values of α fitted along with β in Figure 4, the magnitude of the errors $\pm\Delta\alpha$ were larger than the range of values of α. In order to get the precision of α down to reasonable levels, the quality of the fit must be excellent ($R^2 \geqslant 0.99$). The reason why such high quality fits are required is possibly due to the fact that the theoretical curves are rapidly changing in only a few θ regions, (e.g., 160°–190° range, see Figure 2) so a small change in data in this range can result in a horizontal shift of the best fit values by a couple of degrees. Precise measurement of both 2 f and dc components at each θ point are thus essential. This is compounded by the fact that changes in α will likely be small in biological media. Work is in progress to improve the determination of optical rotation. It is important to determine α accurately, as it would likely yield useful information on the amount of chiral material in the sample, which could be useful in applications such as the measurement of glucose, or other chiral molecules in tissue. Knowing α, one may be able to estimate the concentration of chiral molecules if the path length were known, or vice versa, since chiral molecules produce a characteristic amount of rotation per unit path length per unit concentration.

A large source of background noise is stray laser light, created by interference and scattering effects from the various optical devices in the beam path. This effect made it difficult to obtain a precise value for β at high optical densities in Figure 4, and possibly played a role in optical rotation fluctuations. Encouragingly for potential biomedical use, electronic noise and ambient (nonlaser) lighting did not appreciably interfere with the results. As implemented, the synchronous detection technique using lock-in amplification is excellent at negating the effects of these noise sources.

An important area for future investigation is the sensitivity of the system to the exact value of the detection angle. In other words, is there also significant polarization preservation in directions close to, but not exactly 180°? Theoretical results have indicated that the exact backscattering direction has unique polarization preservation properties within a very narrow angular range (~20 mrad),[6–10,15,16] and it will be worth studying whether this holds true in tissues and in phantoms. If it does not, and a reasonable polarization fraction is preserved within a $\geqslant$5° cone around 180°, then the use of a beamsplitter may not be necessary. This would simplify both the theory and the measurements.

6 Conclusions

Methods for measuring and analyzing polarized light backscattered from turbid media have been developed. Reasonable agreement between the theory and the experimental data is demonstrated in both nonbiological and biological turbid media, including *in vivo* tissues. It is shown that some polarized light will survive at high optical densities in the exact backscattering direction, a finding of potential biomedical importance for examination of highly scattering tissues. The previously reported chirality enhanced polarization preservation is not noticeable in the backscattering direction in microsphere phantoms. Results from biological tissues suggest that these types of polarization measurements may contain useful information, as over 10% of the incident polarization is preserved in both *in vivo* human and *ex vivo* beef samples.

Acknowledgments

We wish to acknowledge Dr. Kai Zhang for providing electronic assistance, and the Natural Science and Engineering Research Council of Canada for funding this research.

References

1. *Optical-Thermal Response of Laser-Irradiated Tissue*, A. J. Welch and M. J. C. van Gemert, Eds., pp. 275–300, Plenum, New York (1995).
2. See, for example, feature issue on ''Diffusing photons in turbid media,'' *Appl. Opt.* **36**, 9–231 (1997).

3. See, for example, feature issue on ''Optical coherence tomography,'' *Opt. Express* **3**, 114–235 (1998).
4. *Handbook of Biological Confocal Microscopy*, J. B. Pawley, Ed., 2nd ed., Plenum, New York (1995).
5. See, for example, *OSA Trends in Optics and Photonics, Biomedical Optical Spectroscopy and Diagnostics/Therapeutic Laser Applications*, E. M. Sevick-Muraca, J. A. Izatt, and M. N. Ediger, Eds., Vol. 22, OSA, Washington, DC (1998).
6. M. P. van Albada and A. Lagendijk, ''Observation of weak localization of light in a random medium,'' *Phys. Rev. Lett.* **55**, 2692–2695 (1985).
7. P. E. Wolf and G. Maret, ''Weak localization and coherent backscattering of photons in disordered media,'' *Phys. Rev. Lett.* **55**, 2696–2699 (1985).
8. F. C. MacKintosh, J. X. Zhu, D. J. Pine, and D. A. Weitz, ''Polarization memory of multiply scattered light,'' *Phys. Rev. B* **40**, 9342–9345 (1989).
9. R. Berkovits and M. Kaveh, ''The vector memory effects for waves,'' *Europhys. Lett.* **13**, 97–100 (1990).
10. A. S. Martinez and R. Maynard, *Photonic Band Gaps and Localization*, C. M. Souloukis, Ed., pp. 99–114, Plenum, New York (1993).
11. M. Dogariu and T. Asakura, ''Photon pathlength distribution from polarized backscattering in random media,'' *Opt. Eng.* **35**, 2234–2239 (1996).
12. M. P. Silverman, W. Strange, J. Badoz, and I. A. Vitkin, ''Enhanced optical rotation and diminished depolarization in diffusive scattering from a chiral liquid,'' *Opt. Commun.* **132**, 410–416 (1996).
13. J. M. Schmitt, A. H. Gandjbakhche, and R. F. Bonner, ''Use of polarized light to discriminate short-path photons in a multiply scattering medium,'' *Appl. Opt.* **31**, 6535–6546 (1992).
14. I. A. Vitkin and E. Hoskinson, ''Polarization studies in multiply scattering chiral media,'' *Opt. Eng.* **39**, 353–362 (2000).
15. C. Brosseau, *Fundamentals of Polarized Light: a Statistical Optics Approach*, Wiley, New York (1998).
16. A. Dogariu, C. Kutsche, P. Likamwa, G. Boreman, and B. Moudgil, ''Time-domain depolarization of waves retroreflected from dense colloidal media,'' *Opt. Lett.* **22**, 585–587 (1997).
17. L. D. Barron, *Molecular Light Scattering and Optical Activity*, Cambridge Press, London, UK (1982).
18. A. Lakhtakia, *Beltrami Fields in Chiral Media*, World Scientific Publishing, Singapore (1994).
19. M. P. Silverman, *Waves and Grains*, Princeton University Press, Princeton, NJ (1997).
20. M. P. Silverman and W. Strange, ''Object delineation within turbid media by backscattering of phase-modulated light,'' *Opt. Commun.* **144**, 7–11 (1997).
21. J. C. Kemp, ''Piezo-optical birefringence modulators: new use for a long-known effect,'' *J. Exp. Theor. Phys.* **59**, 950–954 (1969).
22. M. P. Silverman, N. Ritchie, G. M. Cushman, and B. Fisher, ''Experimental configurations using optical phase modulation to measure chiral asymmetries in light specularly reflected from a naturally gyroptopic medium,'' *J. Opt. Soc. Am. A* **5**, 1852–1863 (1988).
23. E. Collett, *Polarized Light: Fundamentals and Applications*, Marcel Dekker, New York (1993).
24. S. L. Jacques, M. R. Ostermeyer, L. Wang, and D. V. Stephens, ''Polarized light transmission through skin using video reflectometry: toward optical tomography of superficial tissue layers,'' *Proc. SPIE* **2671**, 199–210 (1996).
25. A. H. Hielscher, J. R. Mourant, and I. J. Bigio, ''Influence of particle size and concentration on the diffuse backscattering of polarized light from tissue phantoms and biological cell suspensions,'' *Appl. Opt.* **36**, 125–135 (1997).
26. B. D. Cameron, M. J. Rakovic, M. Mehrubeouglu, G. Kattawar, S. Rastegar, L. V. Wang, and G. L. Cote, ''Measurement and calculation of the two-dimensional backscattering Mueller matrix of a turbid medium,'' *Opt. Lett.* **23**, 485–487 (1998).
27. It is possible to propose Mueller matrices that differ from the suggested depolarization matrix (nonzero elements at $M_{11}=1$, $M_{22}=M_{33}=M_{44}=\beta$). For example, to account for different depolarization rates of linearly versus circularly polarization states, a matrix with nonzero elements at $M_{11}=1$, $M_{22}=M_{33}=\beta_l$, $M_{44}=\beta_c$ may be more appropriate (β_l = degree of linear polarization, β_c = degree of circular polarization, $\beta=(\beta_l^2+\beta_c^2)^{1/2}$ = total degree of polarization), although this representation is nonunique as well. It can also be argued that the current one-β-parameter depolarization description is correct, and that the total degree of polarization β obtained from the data fits is further decomposable into β_l and β_c as done in Ref. 12. For the current study, the suggested form of the Mueller depolarization matrix is valid in that the contribution of M_{44}, whether same or different from M_{22} and M_{33}, does not propagate to the final signal expression of Eq. (7).
28. M. Abramowitz and I. A. Stegun, *Handbook of Mathematical Functions*, p. 361, Dover, New York (1965).
29. T. C. Oakberg, ''Modulated interference effects: use of photoelastic modulators with lasers,'' *Opt. Eng.* **34**, 1545–1550 (1995).
30. C. F. Bohren and D. R. Huffman, *Absorption and Scattering of Light by Small Particles*, Wiley, New York (1983).
31. V. Sankaran, M. J. Everett, D. J. Maitland, and J. T. Walsh, Jr., ''Comparison of polarized-light propagation in biological tissue and phantoms,'' *Opt. Lett.* **24**, 1044–1046 (1999).